Synthesis and Self-Assembly of Spin-Labile and Redox-Active Manganese(III) Complexes

Claudio Gandolfi,[a] Tatiana Cotting,[a] Paulo N. Martinho,[b] Olha Sereda,[c] Antonia Neels,[c] Grace G. Morgan[b] and Martin Albrecht*[a,b]

Received (in XXX, XXX) Xth XXXXXXXXX 200X, Accepted Xth XXXXXXXXX 200X
First published on the web Xth XXXXXXXXX 200X
DOI: 10.1039/b000000x

New amphiphilic and spin-labile Mn^{III} complexes based on dianionic N_4O_2-hexadentate sal_2trien or sal_2bapen ligands were prepared that contain OC_6H_{13}, $OC_{12}H_{25}$, or $OC_{18}H_{37}$ alkoxy substituents at different positions of the salicylidene unit (H_2sal_2trien = *N,N'''*-bis(salicylidene)-1,4,7,10-tetraazadecane, H_2sal_2bapen = *N,N'''*-bis(salicylidene)-1,5,8,12-tetraazadodecane). According to electrochemical measurements, these complexes undergo two (quasi)reversible redox processes. Temperature-dependent magnetic measurements revealed a high-spin configuration for all sal_2trien complexes (S = 2) and gradual spin crossover for sal_2bapen complexes from high to low spin (S = 1). The chain length strongly influences the spin crossover, as C_{18}-functionalization stabilizes the low spin state at much higher temperature than shorter alkyl chains. Moreover, long alkyl chains allow for spontaneous self-assembly of the molecules, which was investigated in single crystals and in Langmuir-films at the air-water interface. Long alkyl chains (C_{12} or C_{18}) as well as a mutual *syn*-orientation of these molecular recognition sites were required for the Langmuir monolayers to be stable.

Introduction

Interest in complexes that undergo spin crossover (SCO) has been growing considerably during recent years because SCO-active materials show great potential for application as memory storage and processing devices.[1] Ideally, the spin change is abrupt and displays hysteresis features to entail bistability over a given temperature range.[2] Such behavior is related to high cooperativity of the spin-labile metal centers, induced for example by intermolecular interactions like hydrogen bonding, π–π stacking, and electrostatic interactions. Hence supramolecular principles[3] may be particularly efficient for engineering and optimizing cooperativity. A few (self-)assembly approaches have been explored thus far for organizing spin-labile centers either in the solid state,[4] in nanoparticles,[5] in gels,[6] and recently even in solution.[7]

While most of these studies have involved spin-labile iron or cobalt centers, only little is known about engineering manganese(III) complexes for self-assembly.[8] This is remarkable, especially when considering the significant potential of managanese(III) centers as active sites of switches due to their high degree of electronic and magnetic variability. Manganese(III) centers undergo facile one-electron oxidations and reductions at relatively low potential costs, and the metal d^4 electronic configuration presets such complexes for spin crossover. However, only a few SCO-active manganese(III) systems are known.[9] A possible reason for the limited accessibility of SCO-active manganese complexes may be the difficulty associated with preparing configurationally stable low-spin complexes.[10] In the few complexes that exhibit SCO activity, the manganese center is often ligated by a multidentate ligand.[11] For example, complex **I** comprising a dianionic hexadentate N_4O_2 ligand framework was reported to undergo a thermally induced spin transition from S = 2 to S = 1 (Fig. 1).[12] Based on our previous achievements in self-assembling iron(III) and cobalt(III) complexes comprising a related N_4O_2 ligand system,[13] the functionalization of complexes related to **I** with aliphatic chains therefore constitutes an obvious approach for synthesizing amphiphilic species that may show both, (electro)magnetically activity and high propensity to (self-)assemble. These two properties, functionality and assembly, are key factors for the development of new functional devices.

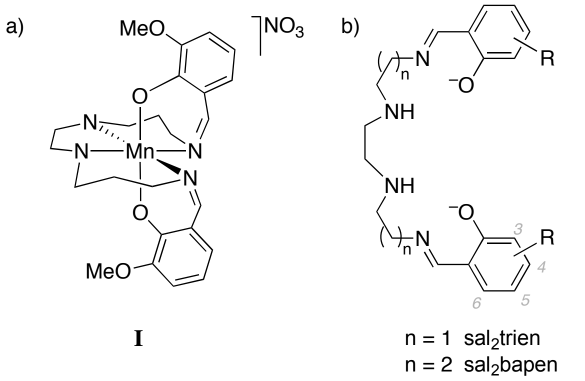

Fig. 1 a) SCO-active Mn(3-MeO-sal_2bapen) complex **I**; b) ligand frameworks used in this work, including generalized carbon labeling scheme for introducing substituents R at the phenolic ring

Here we report on new SCO active manganese(III) complexes and on the implications of aliphatic ligand functionalization. Specific attention has been directed towards the influence of the hydrophilic-lipophilic ratio on the chemical properties (SCO and redox activity) and on the propensity of the complexes to self-assemble. Variation of the

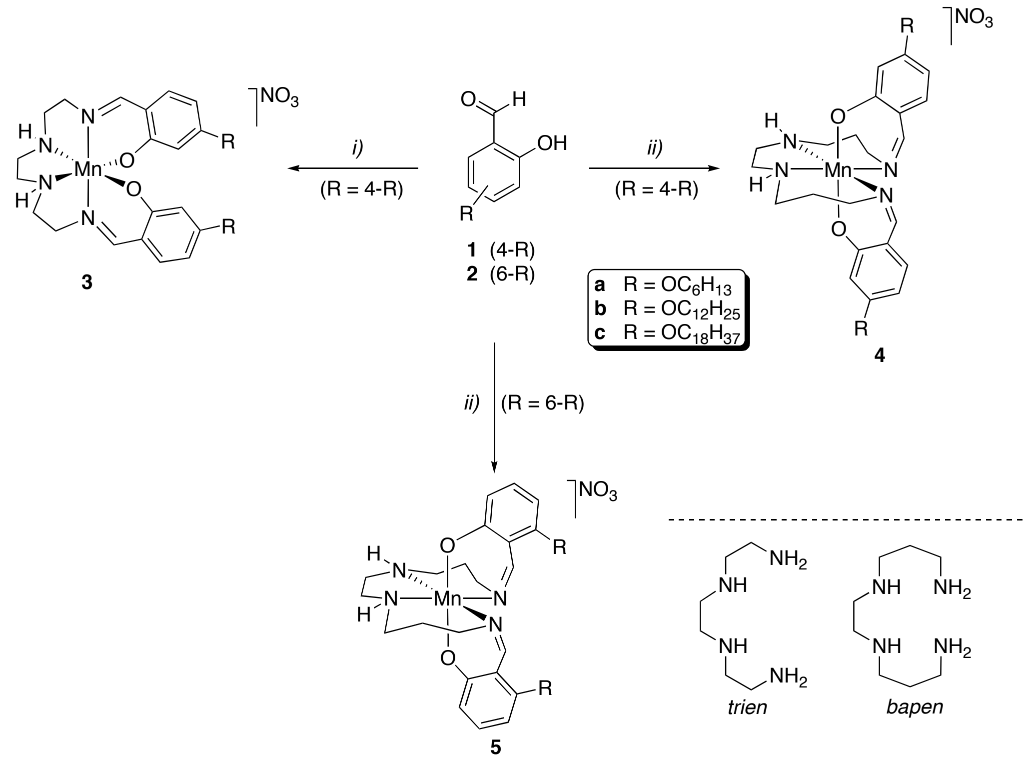

Scheme 1 Synthesis of complexes **3–5**; reagents and conditions: *i)* trien, NaOMe, $Mn(NO_3)_2$ hydrate, air, EtOH/THF (2:1 v/v), 60 °C, 0.5 h; *ii)* bapen, NaOMe, $Mn(NO_3)_2$ hydrate, air, EtOH/THF (2:1 v/v), RT, 0.5 h.

hydrophilic-lipophilic balance has been performed by modifying the skeleton of the hexadentate N_4O_2 ligand and by introducing alkyl chains of different length. Distinct trends have emerged from these studies that may serve as guidelines for further device fabrications using related SCO-active manganese(III) complexes.

Results and discussion

Synthesis of manganese(III) complexes

The amphiphilic manganese(III) complexes **3** comprising a sal$_2$trien ligand framework functionalized with two alkyl chains were prepared according to modified literature procedures.[14] Thus, condensation of the known[15] alkoxy-substituted salicylaldehydes **1** with triethylenetetramine (trien) followed by *in situ* metallation with manganese(II) nitrate in the presence of NaOMe afforded, after standing in air, the oxidized green manganese(III) complexes **3** (Scheme 1). A related protocol using *N,N'''*-bis(3-aminopropyl) ethylenediamine (bapen) instead of trien yielded the alkyl-tailed purple complexes **4** and **5**. All products were purified by flash chromatography and, if required, by repetitive precipitation. The complexes containing the sal$_2$bapen ligand scaffold (complexes **4** and **5**) consistently showed better solubility in organic solvents than their sal$_2$trien analogs **3**, indicating a distinct influence of the alkyl linker between the amine and imine coordination sites.

Different spectroscopic analyses allowed the influence of ligand modifications to be examined. Infrared spectroscopy on complexes **3–5** revealed only slightly reduced energies of the strong $\nu_{C=N}$ absorption bands around 1600 cm^{-1} ($CHCl_3$ solution) as compared to the analogous non-alkylated complexes,[16] Similarly, the bands between 1524–1595 cm^{-1}, assigned to aromatic C=C vibrations,[16a] remain essentially unaltered. A characteristic shift of the $\nu_{C=N}$ band towards higher energy was noted upon expanding the ligand skeleton from sal$_2$trien to sal$_2$bapen (average $\nu_{C=N}$ 1591 cm^{-1} in complexes **3** *vs.* 1605 cm^{-1} in **4** and 1615 cm^{-1} in **5**), indicating that the C=N bond is influenced by both, the *trans* coordinated ligand (*cf.* **3** and **4**) and the aromatic substitution pattern (*cf.* **4** and **5**).

The UV-vis spectra of all complexes display strong charge transfer and intraligand π-π* transitions below 400 nm. In addition, the sal$_2$trien complexes **3** feature a shoulder at 480 nm (ε = 1700 M^{-1}cm^{-1}) originating from phenolate-to-manganese LMCT transitions, and a very broad and weak d-d absorption band around 640 nm (ε = 330 M^{-1}cm^{-1}).[17] These general features do not vary significantly upon changing the alkyl chain length (**3a–3c**) and they are strongly related to those of analogues lacking alkoxy groups.[16c] The absorption maxima of the sal$_2$bapen complexes **4–5** are shifted to lower energy as compared to **3**. The LMCT band appears at around 510 nm (ε = 780 and 1100 M^{-1}cm^{-1} for **4** and **5**, respectively) and a very weak shoulder is observed around 660 nm (ε = 210 M^{-1}cm^{-1}).

Electrochemistry

Cyclic voltammetry (CV) measurements of complexes **3–5** (CH_2Cl_2 solutions) in the –1.2 V to +1.2 V potential range

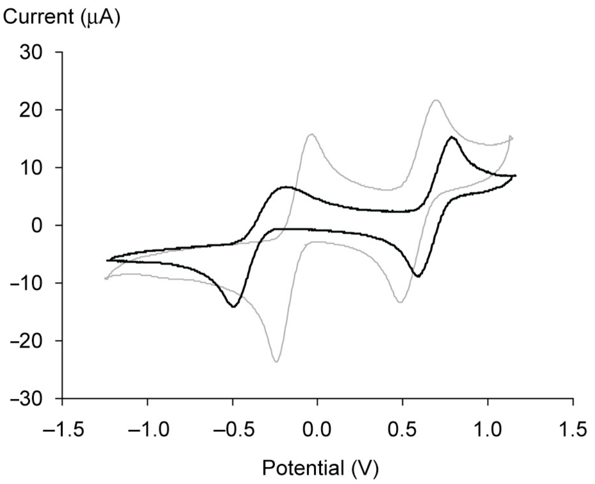

Fig. 2 Representative cyclic voltammogram (second cycle) showing the Mn^{3+}/Mn^{2+} reduction and the Mn^{4+}/Mn^{3+} oxidation of complexes **3a** (grey) and **5a** (black).

Table 1 Electrochemical Data of Manganese(III) Complexes [a]

Complex	Mn^{4+}/Mn^{3+}		Mn^{3+}/Mn^{2+}			
	$E_{1/2}$' /V	ΔE' /mV	E_{pc} /V	E_{pa} /V	$E_{1/2}$ /V	ΔE /mV
3a	+0.59	197	−0.25	−0.02	−0.14	216
3b	+0.63	207	−0.23	−0.02	−0.13	212
3c	+0.58	202	−0.25	−0.02	−0.14	226
4a	+0.64	160	−0.48	−0.05	---	438
4b	+0.66	169	−0.53	−0.01	---	517
4c	+0.66	226	−0.54	−0.05	---	494
5a	+0.69	160	−0.45	−0.25	−0.35	207
5b	+0.68	174	−0.46	−0.24	−0.35	221
5c	+0.70	117	−0.44	−0.26	−0.35	179

[a] CH_2Cl_2 solution, 0.1 M *n*-Bu_4PF_6 as supporting electrolyte; $E_{1/2}$ *vs* SCE, Pt working electrode, scan rate 100 mV s^{-1}; Fc^+/Fc ($E_{1/2}$ = +0.46 V) or $[Ru(bpy)_3]^{3+}/[Ru(bpy)_3]^{2+}$ ($E_{1/2}$ = +1.39 V) as internal standard.

indicated that reduction as well as oxidation of the complexes is accessible at moderate potential (Table 1).[17] Quasi-reversible oxidation occurred for all complexes in a narrow potential window. The oxidation potentials suggest a small yet distinct modulation of the donor properties of the N_4O_2 ligand set, decreasing in the sequence **3** ($E_{1/2}$ 0.60) > **4** ($E_{1/2}$ 0.65) > **5** ($E_{1/2}$ 0.69).[18] These differences may be a consequence of the size of the metallacycle and of the alkoxide substitution pattern. No specific effect of the alkyl chain length on the oxidation potential was noted. Stronger disparities were observed for the Mn^{3+} to Mn^{2+} reduction in the three types of complexes. The reduction potentials for the sal$_2$bapen complexes **4** and **5** are about 200 mV more negative than those of complexes **3**. Hence, both the Mn^{4+} and the Mn^{2+} state are more easily accessible for complex **3** as compared to the sal$_2$bapen complexes **4** and **5** (Fig. 2). Different reduction behavior may originate from modulation of the strain imposed by the ligand framework (five- *vs* six-membered metallacycles), or from modification of the donor group arrangement (*cis*- *vs* *trans*-positioned oxygens). Moreover, the relatively high anodic peak potential E_{pa} in complex **4** paired with the low maximum peak current i_{pa} indicate a more complex process than simple re-oxidation of electrochemically generated Mn^{2+} to Mn^{3+}. Although Mn^{3+}

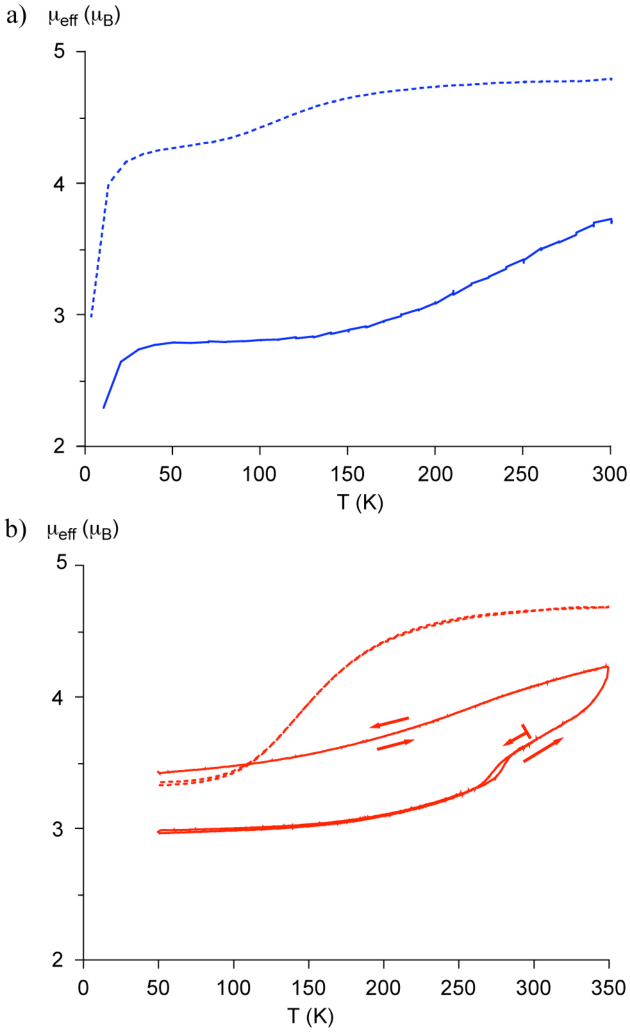

Fig. 3 Temperature-dependence of the magnetic moment μ_{eff} (μ_B) of complexes **4a** × 0.75 acetone and **4c** (a) and of **5a** × H_2O and **5c** (b); dashed lines refer to OC_6H_{13} tails, solid lines to $OC_{18}H_{37}$ tails.

reduction was previously reported to be reversible,[19] our results provide further support that the electrochemically generated Mn^{2+} species is not stable.[14,20]

Magnetism

The magnetic properties of selected complexes have been investigated over a temperature range of 300–50 K. Akin to related complexes,[12] crystalline samples of **3a** × 1.75 H_2O and **3c** displayed a temperature-independent magnetic moment (μ_{eff} = 4.85 and 4.56 μ_B, respectively).[21] This value is in agreement with the expected spin-only magnetic moment calculated for a high spin complex with four unpaired electrons (S = 2, μ_{eff} = 4.90 μ_B). The hexyloxy bapen complexes **4a** and **5a** both exhibit a spin transition. Complex **4a** shows a gentle and incomplete SCO between 150 and 50 K with $T_{1/2}$ around 100 K. The low temperature μ_{eff} = 4.33 μ_B corresponds to an approximate 1:3 distribution of low spin/high spin manganese centers.

The transition for crystalline **5a** × H_2O is more pronounced, falling from almost 100% high spin at RT (μ_{eff} = 4.65 μ_B) to μ_{eff} = 3.32 μ_B at 120 K (Fig. 3b, $T_{1/2}$ ca. 150 K). The measured

Table 2 Selected bond lengths (Å) for complexes **3a**, **4a**, and **5a** at 173 K

	3a		4a		5a
M =	Mn1	Mn2	Mn1	Mn2	Mn1
M–O1	2.062(10)	2.016(11)	1.895(6)	1.870(6)	1.879(2)
M–O2	1.909(11)	1.914(11)	1.850(7)	1.902(6)	1.873(2)
M–N1 $_{imine}$	2.004(12)	1.978(13)	2.034(8)	2.038(9)	2.068(3)
M–N2	2.296(11)	2.245(13)	2.275(6)	2.215(9)	2.142(3)
M–N3	2.118(11)	2.176(12)	2.201(8)	2.250(8)	2.145(3)
M–N4 $_{imine}$	1.939(16)	1.961(13)	2.159(8)	2.083(10)	2.045(3)
Σ [a]	68.1	64.4	62.9	71.8	54.5

[a] angular distortion parameter Σ calculated according to ref. 24.

low spin magnetic moment is higher than that expected for two unpaired electrons (μ_{eff} = 2.82 μ_{B} for S = 1), suggesting that about 2/3 of the molecules have changed configuration. No distinct color change has been noted upon SCO.

The magnetic moments of the OC_{18}-functionalized complexes **4c** and **5c** are lower at RT (μ_{eff} = 3.74 μ_{B} and 3.65 μ_{B}, respectively; Fig. 3b). They decrease gradually upon cooling and reach a plateau at μ_{eff} = 2.85 μ_{B} and 2.98 μ_{B}, respectively, consistent with the S = 1 state.[22] Complex **4c** adopts a low spin configuration only below 60 K, whereas **5c** is low spin up to 220 K. The relatively low magnetic moment of these complexes at room temperature suggests a mixture of high and low spin centers at this temperature.[23] Upon heating a sample of **5c** to 350 K the μ_{eff} indeed increases to μ_{eff} = 4.24 μ_{B}, indicating a predominantly S = 2 configuration. Accordingly, the spin transition is centered just around 295 K which would be very attractive for further processing. After heating, however, only a small fraction converted to the low spin state (μ_{eff} = 3.49 μ_{B} at 100 K). Warming of complex **5c** hence disables SCO, perhaps because of a modified packing of the complexes due to the presence of long alkyl chains.[24] Such a hypothesis is supported by the similar behavior of the warmed sample and an amorphous sample of **5c**.[25] Nevertheless, we observe that long alkyl chains tend to stabilize the less common S = 1 configuration of manganese(III) centers.[26]

Solid state molecular structures

Single crystals of complexes **3a**, **4a**, and **5a** were subjected to an X-ray diffraction analysis. The global structures (Fig. 4) are consistent with previous studies on related complexes.[14,16,19,20] Complex **3a** features *cis*-positioned phenolate oxygens, whereas in complexes **4a** and **5a**, the oxygen atoms are in mutual *trans* arrangement. Generally a significant distortion from an ideally octahedral geometry is noted in all complexes, which may be reflected by the significant distortion parameter Σ (Table 2).[27]

The asymmetric unit of **3a** is composed of two unique complex cations, which each show a Jahn-Teller elongation along one of the amine nitrogens and one of the phenolate oxygens (Table 2). Generally, bond lengths and angles are consistent with a high spin configuration at the Mn^{III} center as deduced from magnetic measurements (*vide supra*).[21] The alkyl chains are fully stretched and in a mutually cisoid arrangement. The dihedral angle α between the two phenolate rings in each complex is about 117°. Values of α above 90° have been suggested to preclude SCO activity in Fe(sal_2trien) complexes.[28] This criterion might be less relevant for the manganese series, since the equally spin-stable methoxy-substituted analog of **3a** has α = 87.8.[12]

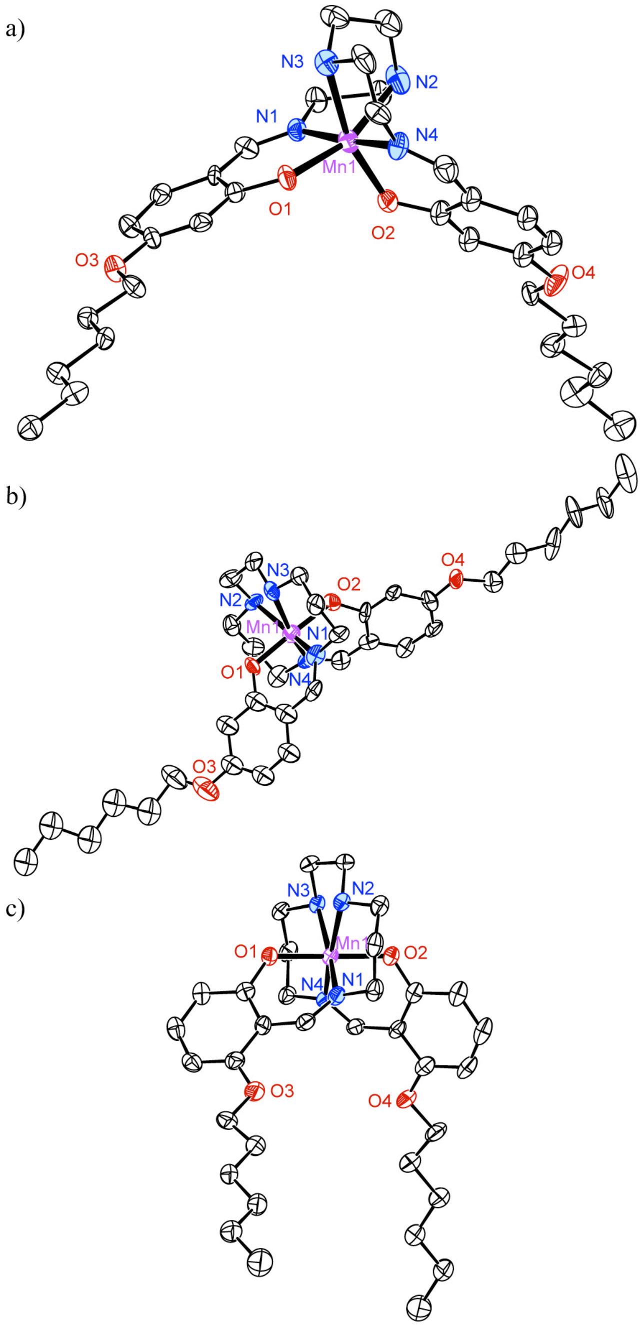

Fig. 4 ORTEP representations of the Mn^{III} complex cations **3a** and **4a** (a and b, respectively, 30% probability ellipsoids, only one of the two independent residues shown), and **5a** (c, 50% probability ellipsoids). All hydrogen atoms, cocrystallized solvent molecules, and non-coordinating anions are omitted for clarity.

The unit cell of **4a** comprises two independent complexes that are nearly identical. Each has more regular geometry than that in **3a**. The shorter Mn–O distances and the longer M–N bonds compared to **3a** reflect the predominantly HS state with population of the $d_{x^2-y^2}$ orbital producing an axial compression.

Upon displacing the alkoxy chain to the imine *ortho* position (**5a**, Fig. 4c) the M–N_{amine} distance decreases considerably (2.14 Å *vs*. > 2.20 Å in **4a**), in line with the lower population of HS sites for **5a** at 173 K. Otherwise, only little changes were observed for the M–O and M–N_{imine} bond lengths. While most of the bond lengths in **5a** at 173 K are similar to those in the methoxy-functionalized complex **I** at RT, which is known to be in high spin configuration, partial spin crossover may be supported by the short M–N_{amine} bonds in **5a**. In addition, the angular distortion parameter (Σ = 54.5) is between the parameters calculated for the high and the low spin states of complex **I** (70.7 and 45.0, respectively),[12] and suggests neither a clear HS nor LS configuration (*cf* magnetic data above).

Crystal packing

In all measured crystals, a hydrogen bonding motif was detected that involves one or both of the ligand N-H bonds. For example in crystals of **3a**, each unique complex cation forms a hydrogen bond *via* the amine hydrogen to a nitrate oxygen, which presumably also acts as acceptor for a co-crystallized water molecule (hydrogen atoms could not be located). This water molecule in turn is ideally placed for acting as hydrogen bond acceptor from another N–H unit, thus resulting in a dimeric structure that is interlinked via a N–H$\cdots O_{nitrate}\cdots$H–$O_{water}\cdots$H–N motif.[21] The two inequivalent complex cations of **4a** also form a dimeric structure due to N–H$\cdots$ON(O)O$\cdots$H–N interactions of the amine-bound hydrogens to two oxygen atoms of the nitrate counterion. Complexes of **5a** are linked together by a similar hydrogen bonding motif as **3a**, involving a NO_3^- counterion and a co-crystallized H_2O molecule. Hence, hydrogen bond formation between the ligand N-H group and the NO_3^- anion seems to constitute a general feature that may also become useful for crystal engineering. In contrast to the previously discussed structures, the hydrogen bonding in **5a** includes both N–H bonds of the cationic complex and hence results in the formation of a polymeric 1D-chain rather than dimeric structures as in **3a** and **4a**.

In addition to the hydrogen bonding, crystal packing analysis of **3a** also revealed a highly anisotropic arrangement of the complex cations. Alignment of the alkyl chains along the crystallographic c-axis produces alternating apolar and polar layers within the crystallographic ab-plane (Fig. 5a). The layers are assembled in head-to-head and tail-to-tail arrangement, thus resulting in the formation of a well-defined 3-dimensional assembly comprising hydrophilic and hydrophobic lamellar domains that are about 9.1 and 14.9 Å thick, respectively. The alkyl chains are densely packed and are separated by about 4 Å.[29] Hence, lipophilic interactions may further stabilize the molecular packing in **3a**. In contrast, cations of **4a** are arranged in perpendicular orientation and do not feature any specific alignment of the alkyl chains nor distinct hydrophilic and hydrophobic domains (Fig. 5b).

The packing of **5a** shows, similar to **3a**, a layered structure (Fig. 5c). As a consequence of the nearly orthogonal alignment of the alkyl chains within each complex, the aliphatic tails of adjacent layers are strongly interdigitated. Hence double layer formation is much less pronounced and the interplanar distance is only 12.4 Å and hence considerably smaller than in crystals of **3a**.

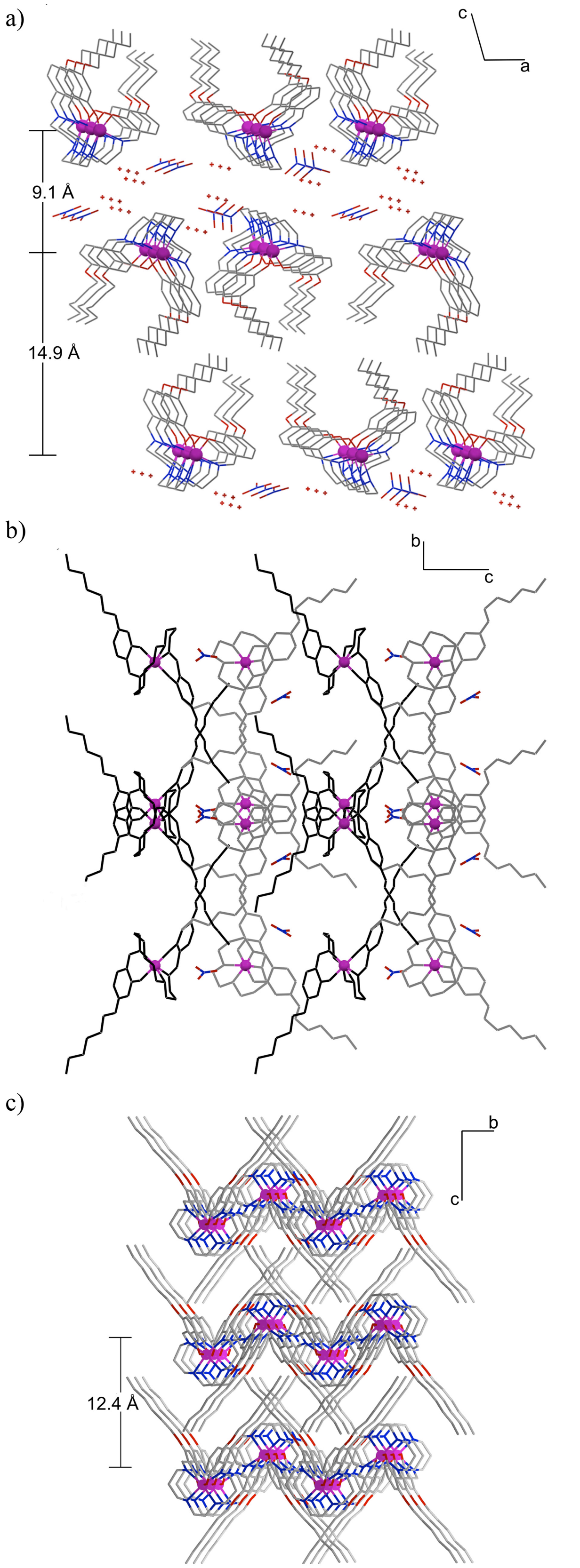

Fig. 5 Crystal packing of the complexes: (a) projection of **3a** along the b-axis; (b) projection of **4a** along the a-axis; (c) projection of **5a** along the

a-axis (nitrate and water residue omitted for clarity); color code: carbon (grey), nitrogen (blue), oxygen (red), manganese (purple).

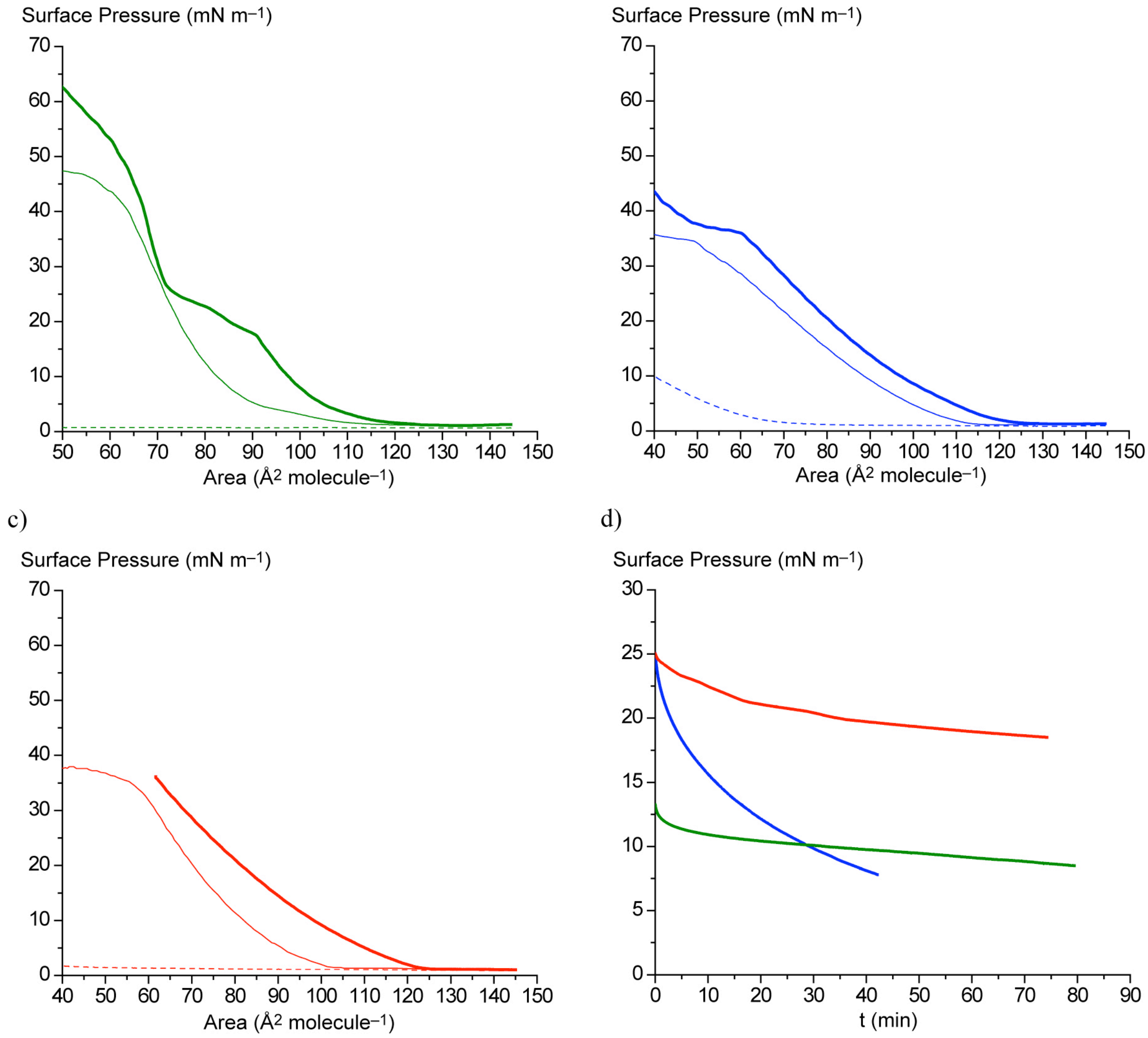

Fig. 6 Chain length dependence of the isotherm plots of Langmuir monolayers of complexes **3** (a), **4** (b), and **5** (c), different alkoxy substituents are represented by dashed (OC_6H_{13}), solid ($OC_{12}H_{25}$), or bold lines ($OC_{18}H_{37}$); (d) film stability over time of monolayers composed of **3c** (green), **4c** (blue), and **5c** (red).

Evaluation of the shortest metal-metal distance indicates that this parameter is not decisive for inducing SCO. In spin-labile **5a**, the manganese(III) centers are separated by 9.153 Å within one layer. This distance is significantly larger than the closest intermetallic contact in crystals of complex **I** (8.914 Å in HS state and 8.411 Å in LS). The Mn···Mn separation in spin-stable complexes **3a** and **4a** is even smaller, 7.443 Å and 8.189 Å, respectively.[30] Tentatively, the SCO activity of **5a** may thus be attributed to the ordered interdigitation of the alkyl chains and the consequentially short layer separation, perhaps in combination with the hydrogen bonded 1D network, which interconnects complexes of different layers.

Self-assembly at interfaces

Langmuir-Blodgett (LB) film fabrication provides an elegant tool for arranging molecules at the supramolecular level and offers the possibility to sequentially deposit molecular monolayers with high precision and reproducibility.[31] The assembly of amphiphilic molecules with a specific function can thus afford mono- and multilayered films,[32] and hence offers an attractive methodology for device fabrication.[33] These attractive features prompted us to investigate the potential of of complexes **3–5** to form Langmuir films at the air-water interface. Representative pressure-area isotherms revealed that complexes with C_{12} and C_{18} alkyl tails self-assemble into densely packed Langmuir monolayers, which collapse typically at a surface area slightly below 70 $Å^2$/molecule (Fig. 6). The molecular area in the densely packed film is in good agreement with models based on crystal structure analyses suggesting a surface area of approximately 65(±5) $Å^2$ for the polar heads of **3–5**. When using long chain C_{18}-functionalized complexes, intermolecular contacts establish at an earlier stage of compression than with C_{12}-functionalized complexes. Also the molecular area in compressed C_{18}-functionalized monolayers is larger than with shorter C_{12} tails. Such behavior has been previously observed with analogous iron complexes,[13] and may be due to the increased probability of long chains to backfold. In contrast, the complexes containing hexyloxy substituents did not form monolayers. The apolar section of these molecules is probably too small and thus favors diffusion into the subphase due to partial water solubility or due to micelle formation.

Interestingly, the isotherm of **3c** shows two separated phase transitions at 92 and 72 $Å^2$/molecule, which may point to distinct transitions from liquid expanded to liquid condensed and then to the solid phase. Films built from sal_2trien-type complexes **3** seem to be the most robust in the series measured here, as high surface pressures can be reached (45–60 mN/m *vs*. ca. 35 mN/m for the sal_2bapen-derived species **4** and **5**). In this regime, little changes in the specific area resulted in a marked pressure enhancement, indicating that a solid phase was reached. In contrast, the relative molecular area of monolayers composed of complexes **4b–c** or **5b–c** continuously shrunk upon compression, pointing to a liquid condensed phase. This specific behavior may be a consequence of the reduced hydrophilicity of the sal_2bapen ligand as compared to the sal_2trien system in **3**.

When considering the transoid arrangement of the alkyl tails in complexes **4** and its low tendency to pack into polar and apolar domains (*cf* Fig. 5), it seems surprising that Langmuir monolayer formation with this complex is not significantly different from that of **5** bearing cisoid alkyl chains.[34] Notably, the films composed of complexes **4** are highly unstable (Fig. 6d).[21] In contrast, monolayers composed of **3** and **5** are reasonably stable over extended periods of time (> 80 min) and may thus be used for transfer experiments.

Even though it is generally difficult to extrapolate molecular design to supramolecular organization,[35] especially when using only weak molecular recognition tools such as London forces,[36] complexes **3–5** demonstrate a strong correlation between molecular design, crystal packing, and self-assembling properties. For example, appending the alkoxy tails in a different position on the aromatic ring of sal_2bapen ligands reduces the intramolecular $O_{alkoxy}\cdots O_{alkoxy}$ distance from 11.8 Å in **4a** to 6.7 Å in **5a** (*cf* X-ray structures) and simultaneously modifies the shape of the complex from a linear system (transoid alkyl chains in **4a**) to a U-shaped geometry due to the cisoid arrangement of the alkyl chains. This modification separates the hydrophobic and lipophilic parts sufficiently well to entail the formation of stable films at the air-water interface.[37]

Transfer of the Langmuir films onto supports was of limited success. Only partial transfer was observed due to significant desorption of material during downstrokes, resulting in ill-defined multilayered structures.[21] This drawback may perhaps be resolved by introducing different types of molecular recognition sites for self-assembly and studies along these lines are currently in progress.

Conclusions

Amphiphilic manganese(III) complexes comprising different ligand skeletons were obtained using a simple alkoxy-functionalization approach that allows for adjustment of the hydrophilic-lipophilic balance. The aliphatic chains do not affect the electrochemical properties and allow for accessing three different oxidation states under mild conditions. However, they strongly influence the magnetic behavior of the complexes. Notably, octadecyloxy substituents attached to the sal_2bapen ligand induce $S = 2$ to $S = 1$ spin transitions. Long aliphatic chains stabilize the low spin configuration at much higher temperature (>150 K) as compared to shorter hexyloxy groups. The observation of SCO in the isomeric complexes **4c** and **5c** — the latter with a transition centered around room temperature and hence very attractive for device fabrication—suggests that the inductive character of the alkoxy group is more relevant than mesomeric or steric effects.

Due to the amphiphilic character, the complexes have a high propensity to form distinct hydrophilic and hydrophobic domains upon self-assembly, both in the solid state (crystals) as well as at the air-water interface (Langmuir films). A clear separation between hydrophobic and hydrophilic moieties within the molecular building blocks is essential for the formation of a stable Langmuir monolayer. Since the sal_2bapen framework is considerably less hydrophilic than the sal_2trien analog, the length and the position of the aliphatic chains plays a critical role for inducing self-assembly. Complex **5c** represents an optimized building block, combining SCO lability and redox activity with acceptable Langmuir film stability.

Experimental section

General remarks

The syntheses of the 4-alkoxy-functionalized salicylaldehydes **1**,[15] the 6-alkoxyfunctionalized salicylaldehydes **2**,[21] and the Schiff base, which has been isolated for the preparation of **3c**,[13] were reported elsewhere. THF was dried by passage through a solvent purification column, all other reagents were commercially available and used as received. Flash chromatography was performed using silica gel 60 (63-200 mesh) or basic alox (0.05–0.15 mm, pH 9.5). Melting points were determined using an OptiMelt apparatus (Stanford Research Systems) or a Mettler Toledo TGA/SDTA 851 analyzer and are uncorrected. UV-vis measurements were performed on a Perkin Elmer Lambda 40 instrument in CH_2Cl_2 solution (0.2 mM). IR spectra were recorded on a Mattson 5000 FTIR instrument in $CHCl_3$ solution. UV-vis spectra of LB-films were recorded on a Perkin Elmer Lambda 900 instrument in transmission mode. High resolution mass spectra were measured by electrospray ionization (ESI-MS) on a Bruker 4.7 T BioAPEX II or on a Water Corp. USA Micromass LCT. Elemental analyses were performed at the ETH Zurich (Switzerland) or at the Micronanalytical Laboratory of UCD (Ireland). Electrochemical studies were carried out using an EG&G Princeton Applied Research Potentiostat Model 273A employing a gastight three-electrode cell under an argon atmosphere. A saturated calomel electrode (SCE) was used as reference; a Pt disk (3.14 mm^2) and a Pt wire were used as the working and counter electrode, respectively. The redox potentials were measured in dry CH_2Cl_2 (~1 mM) with n-Bu_4NPF_6 (0.1 M) as electrolyte and ferrocene ($E_{1/2}$ = 0.46 V *vs*. SCE)[38] or $[Ru(bpy)_3][PF_6]_2$ ($E_{1/2}$ =

1.39 V *vs.* SCE)[39] as internal standard. Temperature-dependent magnetization of solid samples was studied using a Quantum Design PPMS system in a temperature range between 300 and 50 K (unless stated otherwise) using an applied field of 0.1 T (**3c**, **4**) or 0.5 T (**3a**, **5**).[40] Susceptibility data were corrected for the diamagnetic contribution calculated from Pascal constants.

Langmuir-Blodgett Films

Pressure-area isotherms and time stability were measured at 25 °C on a KSV MiniMicro Langmuir-Blodgett trough (KSV, Finland) with a surface area between 1700 and 8700 mm^2. Water was purified with a Barnstead Nanopure system (Thermo Scientific), and its resistivity was measured to be higher than 18 MΩ cm. Chloroform (puriss. p.a. ≥ 99.8%, Fluka) was used as spreading solvent. Typically drops of the surfactant solution (20 μL, 0.50 mM) were deposited using a microsyringe on the water subphase. After letting the solvent evaporate for 30 min, the barriers were compressed at 6 mm min^{-1} (3 cm^2 min^{-1}) and the surface pressure was monitored using a platinum Willhelmy plate. Each isotherm has been measured three times with good reproducibility.

Synthesis of complex 3a

Triethylenetetramine (146 mg, 1.0 mmol) was dissolved in EtOH (5 mL) and treated with a solution of **1a** (446 mg, 2.0 mmol) in THF (5 mL). After 5 min, NaOMe (108 mg, 2.0 mmol) was added as a solid and $Mn(NO_3)_2 \times 4H_2O$ (251 mg, 1.0 mmol) in EtOH (5 mL) was added dropwise to the yellow solution. The greenish brown suspension was heated to 60 °C for 30 min open to air and filtered over a bed of silica. The product was eluted with THF (60 mL) and evaporated under reduced pressure. The residue was dissolved in $CHCl_3$ (5 mL) and purified on a short pad of Al_2O_3 (8 cm) by washing first with $CHCl_3$ (100 mL) and subsequent elution with EtOH/THF 2:1 (120 mL). After evaporation of the EtOH/THF fraction, the residue was redissolved in minimum amount of CH_2Cl_2 and centrifuged. The supernatant was precipitated with Et_2O (80 mL) and the precipitation from CH_2Cl_2/Et_2O was repeated once. The precipitate was dissolved in CH_2Cl_2, filtered over Celite, and dried *in vacuo* to give **3a** as a green solid (0.27 g, 40%). Crystals for single crystal structure analysis were grown from slow evaporation of an acetone/water mixture containing **3a**. M.p. 187 °C (decomp.). IR ($CHCl_3$): 1593 ($\nu_{C=N}$), 1524 cm^{-1} ($\nu_{C=C}$). UV-vis (CH_2Cl_2): λ_{max} (ε) = 252 nm (33700 M^{-1}cm^{-1}), 286 nm (27700 M^{-1}cm^{-1}), 321 nm (18800 M^{-1}cm^{-1}), 380 nm (11200 M^{-1}cm^{-1}), 479 nm (1660 M^{-1}cm^{-1}), 599 nm (502 M^{-1}cm^{-1}). HR–MS (ESI): Calcd. for $C_{32}H_{48}MnN_4O_4$ $[M–NO_3]^+$ m/z = 607.3051, found m/z = 607.3058. Anal. found (calcd) for $C_{32}H_{48}MnN_5O_7$ (669.70): C 57.67 (57.39); H 7.14 (7.22); N 10.36 (10.46).

Synthesis of complex 3b

According to the procedure used for **3a**, complex **3b** was obtained from triethylenetetramine (146 mg, 1.0 mmol) in EtOH (5 mL), **1b** (614 mg, 2.0 mmol) in THF (5 mL), NaOMe (108 mg, 2.0 mmol) and $Mn(NO_3)_2 \times 4H_2O$ (251 mg, 1.0 mmol) in EtOH (5 mL) as a green solid (0.34 g, 41%). M.p. 176 °C (decomp.). IR ($CHCl_3$): 1593 ($\nu_{C=N}$), 1523 cm^{-1} ($\nu_{C=C}$). UV-vis (CH_2Cl_2): λ_{max} (ε) = 252 nm (33700 M^{-1}cm^{-1}), 286 nm (27900 M^{-1}cm^{-1}), 321 nm (19200 M^{-1}cm^{-1}), 380 nm (15800 M^{-1}cm^{-1}), 479 nm (1637 M^{-1}cm^{-1}), 606 nm (378 M^{-1}cm^{-1}). HR–MS (ESI): Calcd. for $C_{44}H_{72}MnN_4O_4$ $[M–NO_3]^+$ m/z = 775.4928, found m/z = 775.4917. Anal. found (calcd) for $C_{44}H_{72}MnN_5O_7$ (838.02): C 63.12 (63.06); H 8.69 (8.66); N 8.19 (8.36).

Synthesis of complex 3c

Solid NaOMe (54 mg, 1 mmol) was added to the Schiff base (446 mg, 0.5 mmol) in warm THF (20 mL). After 2 min stirring, a solution of $Mn(NO_3)_2 \times H_2O$ (248 mg, 0.61 mmol) in EtOH (5 mL) was added dropwise. The greenish brown suspension was stirred for 30 min at reflux and filtered over a bed of silica (1.5 cm height). The product was eluted with EtOH /THF 2:1 (100 mL) and dried under reduced pressure. The residue was taken into $CHCl_3$ (5 mL) and purified on a short pad of Al_2O_3 (12 cm) by consecutive elution with $CHCl_3$ (60 mL) and EtOH/THF 2:1 (150 mL). After evaporation of the EtOH/THF fraction, the product was redissolved in $CHCl_3$ (5 mL) and filtered over Celite. The supernatant was evaporated under reduced pressure to give **3c** as a green solid (130 mg, 25%). Analytically pure material was obtained by dissolving **3c** in CH_2Cl_2 (10 mL) and precipitation with Et_2O (70 mL) under stirring. M.p. 198 °C (decomp.). IR ($CHCl_3$): 1586 ($\nu_{C=N}$), 1524 cm^{-1} ($\nu_{C=C}$). UV-vis (CH_2Cl_2): λ_{max} (ε) = 252 nm (32800 M^{-1}cm^{-1}), 286 nm (27400 M^{-1}cm^{-1}), 321 nm (18800 M^{-1}cm^{-1}), 380 nm (10800 M^{-1}cm^{-1}), 481 nm (1750 M^{-1}cm^{-1}), 606 nm (290 M^{-1}cm^{-1}). HR–MS (ESI): Calcd. for $C_{56}H_{96}MnN_4O_4$ $[M–NO_3]^+$ m/z = 943.6812, found m/z = 943.6821. Anal. found (calcd) for $C_{56}H_{96}MnN_5O_7$ (1006.35): C 66.97 (66.84); H 9.61 (9.61); N 6.74 (6.96).

Synthesis of complex 4a

This complex was synthesized according to the method described for **3a**, starting from *N,N'*-bis(3-aminopropyl)ethylenediamine (278 mg, 1.5 mmol) dissolved in EtOH (8 mL), a solution of **1a** (667 mg, 3.0 mmol) in THF (8 mL), NaOMe (162 mg, 3.0 mmol), and $Mn(NO_3)_2 \times H_2O$ (274 mg, 1.5 mmol) in EtOH (5 mL), thus yielding **4a** as a purple solid (0.44 g, 42%). Crystals for single crystal structure analysis were grown by slow evaporation of an acetone/water mixture containing **4a**. M.p. 185 °C (decomp.). IR ($CHCl_3$): 1604 ($\nu_{C=N}$), 1538 cm^{-1} ($\nu_{C=C}$). UV-vis (CH_2Cl_2): λ_{max} (ε) = 251 nm (30400 M^{-1}cm^{-1}), 289 nm (36700 M^{-1}cm^{-1}), 514 nm (790 M^{-1}cm^{-1}), 663 nm (227 M^{-1}cm^{-1}). HR–MS (ESI): Calcd. for $C_{34}H_{52}MnN_4O_4$ $[M–NO_3]^+$ m/z = 635.3369, found m/z = 635.3362. Anal. found (calcd) for $C_{34}H_{52}MnN_5O_7$ (697.76): C 58.25 (58.53); H 7.45 (7.51); N 9.85 (10.04).

Synthesis of complex 4b

According to procedure used for **4a**, the crude title product was obtained from *N,N'*-bis(3-aminopropyl)ethylenediamine (185 mg, 1.0 mmol) in EtOH (5 mL), **1b** (613 mg, 2.0 mmol) in THF (5 mL), NaOMe (108 mg, 2.0 mmol), and $Mn(NO_3)_2 \times H_2O$ (183 mg, 1.0 mmol) in EtOH (5 mL), thus giving **4b** as a purple solid (0.44 g, 51%). M.p. 177 °C (decomp.). IR

($CHCl_3$): 1604 ($\nu_{C=N}$), 1537 cm^{-1} ($\nu_{C=C}$). UV-vis (CH_2Cl_2): λ_{max} (ε) = 251 nm (29400 $M^{-1}cm^{-1}$), 289 nm (36500 $M^{-1}cm^{-1}$), 514 nm (800 $M^{-1}cm^{-1}$), 663 nm (230 $M^{-1}cm^{-1}$). HR–MS (ESI): Calcd. for $C_{46}H_{76}MnN_4O_4$ $[M–NO_3]^+$ m/z = 803.5247, found m/z = 803.5215. Anal. found (calcd) for $C_{46}H_{76}MnN_5O_7$ (866.08): C 63.49 (63.79); H 8.76 (8.85); N 7.85 (8.09).

Synthesis of complex 4c

According to procedure **4a** the crude title product was obtained from *N,N′*-bis(3-aminopropyl)ethylenediamine (185 mg, 1.0 mmol) in EtOH (5 mL), **1c** (613 mg, 2.0 mmol) in warm THF (50 mL), NaOMe (108 mg, 2.0 mmol) and $Mn(NO_3)_2 \times H_2O$ (183 mg, 1.0 mmol) in EtOH (5 mL). Purification was performed on a short pad of Al_2O_3 (13 cm) by consecutive elution with $CHCl_3$ (30 mL) and THF (60 mL). After evaporation of the THF fraction, the product was redissolved in $CHCl_3$ (20 mL) and filtered over Celite. After evaporation of the filtrate under reduced pressure, the residue was recrystallized from warm acetone to give **4c** as a purple solid (0.31 g, 30%). M.p. 187 °C (decomp.). IR ($CHCl_3$): 1607 ($\nu_{C=N}$), 1532 cm^{-1} ($\nu_{C=C}$). UV-vis (CH_2Cl_2): λ_{max} (ε) = 251 nm (29500 $M^{-1}cm^{-1}$), 289 nm (36700 $M^{-1}cm^{-1}$), 512 nm (740 $M^{-1}cm^{-1}$), 663 nm (217 $M^{-1}cm^{-1}$). HR–MS (ESI): Calcd. for $C_{58}H_{100}MnN_4O_4$ $[M–NO_3]^+$ m/z = 971.7120, found m/z = 971.7110. Anal. found (calcd) for $C_{58}H_{100}MnN_5O_7$ (1034.40): C 67.75 (67.35); H 9.81 (9.74); N 6.44 (6.77).

Synthesis of complex 5a

The procedure used for the synthesis of **3a** was used, starting from *N,N′*-bis(3-aminopropyl)ethylenediamine (195 mg, 1.05 mmol) in EtOH (5 mL), **2a** (113 mg, 2.10 mmol) in THF (5 mL), NaOMe (113 mg, 2.10 mmol) and $Mn(NO_3)_2 \times 4H_2O$ (269 mg, 1.05 mmol) in EtOH (5 mL). The dark purple suspension was stirred for 30 min at RT open to air and filtered over a bed of silica. The product was eluted with THF (40 mL) and evaporated under reduced pressure. The residue was dissolved $CHCl_3$ (10 mL) and purified on a short pad of Al_2O_3 (5 cm) by first washing with $CHCl_3$, THF, and finally with EtOH/THF 2:1 (50 mL). After evaporating the EtOH/THF fraction, the residue was repetitively redissolved in CH_2Cl_2 (2 mL) and precipitated with pentane (80 mL) and Et_2O (3 × 80 mL). The residue collected by centrifugation was dissolved in CH_2Cl_2 and filtered over Celite. The filtrate was evaporated *in vacuo* to give **5a** as a purple solid (0.34 g, 46%). Crystals for single crystal structure analysis were grown by slow evaporation of an acetone/water mixture containing **5a**. M.p. 167 °C. IR (CHCl3): 1615 ($\nu_{C=N}$), 1595 ($\nu_{C=C}$), 1556 cm^{-1} ($\nu_{C=C}$). UV-vis (CH_2Cl_2): λ_{max} (ε) = 285 nm (19600 $M^{-1}cm^{-1}$), 320 nm (13900 $M^{-1}cm^{-1}$), 372 nm (5700 $M^{-1}cm^{-1}$), 505 nm (1120 $M^{-1}cm^{-1}$), 666 nm (214 $M^{-1}cm^{-1}$). HR–MS (ESI): Calcd. for $C_{34}H_{52}MnN_4O_4$ $[M–NO_3]^+$ m/z = 635.3364, found m/z = 635.3361. Anal. found (calcd) for $C_{34}H_{52}MnN_5O_7$ (697.76) × 0.5 H_2O: C 57.95 (57.78); H 7.52 (7.56); N 9.81 (9.91).

Synthesis of complex 5b

According to procedure **5a**, the crude title product was obtained from *N,N′*-bis(3-aminopropyl)ethylenediamine (113 mg, 0.61 mmol) in EtOH (3 mL), **2b** (372 mg, 1.21 mmol) in THF (5 mL), NaOMe (66 mg, 1.21 mmol) and $Mn(NO_3)_2 \times 4H_2O$ (155 mg, 0.61 mmol) in EtOH (3 mL). Purification was performed on a short pad of Al_2O_3 (7 cm) by consecutive elution with $CHCl_3$ (100 mL) and THF (50 mL). After evaporation of the THF fraction, the residue was redissolved in acetone (2 mL), and precipitated with pentane (3 × 80 mL). The residue was collected by centrifugation was dissolved in CH_2Cl_2 and filtered over Celite. The filtrate was evaporated *in vacuo* to give **5b** as a purple solid (164 mg, 31%). M.p. 157 °C. IR ($CHCl_3$): 1615 ($\nu_{C=N}$), 1595 ($\nu_{C=C}$), 1556 cm^{-1} ($\nu_{C=C}$). UV-vis (CH_2Cl_2): λ_{max} (ε) = 285 nm (19300 $M^{-1}cm^{-1}$), 320 nm (13500 $M^{-1}cm^{-1}$), 372 nm (5660 $M^{-1}cm^{-1}$), 505 nm (1090 $M^{-1}cm^{-1}$), 666 nm (210 $M^{-1}cm^{-1}$). HR–MS (ESI): Calcd. for $C_{46}H_{76}MnN_4O_4$ $[M–NO_3]^+$ m/z = 803.5242, found m/z = 803.5242. Anal. found (calcd) for $C_{46}H_{76}MnN_5O_7$ (866.07): C 63.50 (63.79); H 8.87 (8.84); N 7.93 (8.09).

Synthesis of complex 5c

According to procedure described for **5a**, complex **5c** was obtained from *N,N'*-bis(3-aminopropyl)ethylenediamine (88 mg, 0.47 mmol) in EtOH (2 mL), **2c** (369 mg, 0.95 mmol) in THF (10 mL), NaOMe (51 mg, 0.95 mmol), and $Mn(NO_3)_2 \times 4H_2O$ (121 mg, 0.47 mmol) in EtOH (3 mL). After column chromatography purification and precipitation, the combined **5c** was obtained as a purple solid (293 mg, 61%). Pure samples for magnetic measurements were prepared by slow evaporation of an acetone solution of **5c**. M.p. 145°C. IR ($CHCl_3$): 1615 ($\nu_{C=N}$), 1595 ($\nu_{C=C}$), 1554 cm^{-1} ($\nu_{C=C}$). UV-vis (CH_2Cl_2): λ_{max} (ε) = 285 nm (19400 $M^{-1}cm^{-1}$), 320 nm (13500 $M^{-1}cm^{-1}$), 372 nm (5690 $M^{-1}cm^{-1}$), 504 nm (1100 $M^{-1}cm^{-1}$), 666 nm (210 $M^{-1}cm^{-1}$). HR–MS (ESI): Calcd. for $C_{34}H_{52}MnN_4O_4$ $[M–NO_3]^+$ m/z = 971.7121, found m/z = 971.7120. Anal. found (calcd) for $C_{58}H_{100}MnN_5O_7$ (1034.40) × 1.5 H_2O: C 65.64 (65.63); H 9.72 (9.78); N 6.47 (6.60).

Crystal Structure Determinations

Suitable single crystals were mounted on a Stoe Mark II-Imaging Plate Diffractometer System equipped with a graphite monochromator. Data collection was performed at –100 °C using Mo-K_α radiation (λ = 0.71073 Å) with a nominal crystal to detector distance of 135 mm. All structures were solved by direct methods using the program SHELXS-97 and refined by full matrix least squares on F^2 with SHELXL-97.[41] The hydrogen atoms were included in calculated positions and treated as riding atoms using SHELXL-97 default parameters. All non-hydrogen atoms were refined anisotropically. A semi-empirical absorption correction was applied for structures **4a** and **5a** using MULABS (PLATON03[42]).

Compound **3a** crystallized with two independent molecules and seven water molecules per asymmetric unit. The absolute structure was determined by refinement of the Flack parameter (0.08(5)).[43] One nitrate anion is disordered and was refined isotropically; the oxygen atoms were split over two positions (occupancies 0.5/0.5). Complex **4a** crystallized with two independent molecules per asymmetric unit. A region of disordered electron density was assumed to be co-crystallised solvent molecules. The absolute structure could be derived with a Flack parameter x = 0.03(3). The SQUEEZE option in PLATON was used to calculate the potential solvent accessible volume in the unit cell: 810 Å^3 was calculated containing about 202 electrons, equated to six acetone molecules (6 × 32 electrons) per unit cell. One nitrate anion is disordered over two positions (occupancies 0.7/0.3). The alkyl chains in **3a** and **4a** suffer from thermal disorder. In the final cycles of refinement their anisotropic displacement parameters were made identical, using the EADP instruction in SHELXL, and the C–C bonds were refined with distance restraints of 1.54(2) Å. Complex **5a** crystallizes with one water molecule per asymmetric unit. Further details on data collection and refinement parameters are collected in the supporting information (Table S-2). Crystallographic data (excluding structure factors) for the structures **3a**, **4a**, and **5a** have been deposited with the Cambridge Crystallographic Data Centre as supplementary publication nos. CCDC 782475-782477. Copies of the data can be obtained free of charge on application to CCDS, 12 Union Road, Cambridge CB2 1EZ, UK [Fax: (int.) +44-1223-336-033; E-mail: deposit@ccds.cam.ac.uk].

Acknowledgments

We thank V. Malik and C. Bernhard (Univ Fribourg) for performing magnetic measurements. This research was supported by ERA-net Chemistry, the Swiss National Science Foundation, and the Alfred Werner Foundation.

Notes and references

[a] *Department of Chemistry, University of Fribourg, Chemin du Musée 9, CH-1700 Fribourg, Switzerland.*
[b] *School of Chemistry & Chemical Biology, University College Dublin, Belfield, Dublin 4, Ireland. Fax: +353 1716 2501; Tel: +353 1716 2504; E-mail: martin.albrecht@ucd.ie*
[c] *XRD Application Lab, CSEM, Rue Jaquet-Droz 1, CH-2002 Neuchâtel, Switzerland.*

† Electronic Supplementary Information (ESI) available: Synthesis of compounds **2a–c**, magnetic measurements of **3a** and **3c**, Langmuir studies (stability plots and multilayering into LB films), and crystallographic details for complexes **3a**, **4a**, and **5a** in CIF format. See DOI: 10.1039/b000000x/

1 (a) O. Kahn and C. J. Martinez, *Science,* 1998, **279**, 44. (b) S. A. Wolf, D. D. Awschalom, R. A. Buhrman, J. M. Daughton, S. von Molnar, M. L. Roukes, A. Y. Chtchelkanova and D. M. Treger, *Science,* 2001, **294***,* 1488. (c) M. Berciu, T. Rappaport and B. Janko, *Nature* 2005, **435**, 71. C. Felser, G. H. Fecher and B. Balke, *Angew. Chem. Int. Ed.,* 2007, **46**, 668. (d) J. J. Parks, A. R. Champagne, T. A. Costi, W. W. Shum, A. N. Pasupathy, E. Neuscamman, S. Flores-Torres, P. S. Cornaglia, A. A. Aligia, C. A. Balseiro, G. K.-L. Chan, H. D. Abruna and D. C. Ralph, *Science,* 2010, **328**, 1370.

2 (a) P. Gütlich, A. Hauser and H. Spiering, *Angew. Chem. Int. Ed. Engl.,* 1994, **33**, 2024. (b) P. Gütlich, Y. Garcia and H. Spiering, in *Magnetism: Molecules to Materials IV*, J. S. Miller and M. Drillon (eds.), Wiley-VCH, Weinheim, Germany, 2002, p 271. (c) P. Gütlich and H. A. Goodwin, *Top. Curr. Chem.,* **2004**, *233*, 1. (d) J.-F. Letard, P. Guionneau and L. Goux-Capes, *Top. Curr. Chem.,* **2004**, *235*, 221. (e) P. J. van Koningsbruggen, Y. Maeda and H. Oshio, *Top. Curr. Chem.,* 2004, **233**, 259.

3 J.-M. Lehn, *Supramolecular Chemistry*, Wiley-VCH, Weinheim, Germany, 1995.

4 (a) J. A. Real, E. Andres, M. C. Munoz, M. Julve, T. Granier, A. Bousseksou and F. Varret, *Science,* 1995, **268**, 265. (b) O. Roubeau, B. Agricole, R. Clerac and S. Ravaine, *J. Phys. Chem. B,* 2004, **108**, 15110. (c) S. Cobo, G. Molnar, J. A. Real and A. Bousseksou, *Angew. Chem. Int. Ed.,* 2006, **45**, 5786. (d) M. Seredyuk, A. B. Gaspar, V. Ksenofontov, Y. Galyametdinov, J. Kusz and P. Gütlich, *J. Am. Chem. Soc.,* 2008, **130**, 1431. (e) S. Cobo, D. Ostrovskii, S. Bonhommeau, L. Vendier, G. Molnar, L. Salmon, K. Tanaka and A. Bousseksou, *J. Am. Chem. Soc.,* 2008, **130**, 9019. (f) Y. Bodenthin, G. Schwarz, Z. Tomkowicz, M. Lommel, T. Geue, W. Haase, H. Möhwald, U. Pietsch and D. G. Kurth, *Coord. Chem. Rev.,* 2009, **253**, 2414. (g) A. B. Gaspar, M. Seredyuk and P. Gütlich, *Coord. Chem. Rev.,* 2009, **253**, 2399. (h) K. E. Funk, M. G. Hilfiger, C. P. Berlinguette, M. Shatruk, W. Wernsdorfer and K. R. Dunbar, *Inorg. Chem.,* 2009, **48**, 3438.

5 (a) T. Forestier, S. Mornet, N. Daro, T. Nishihara, S.-I. Mouri, K. Tanaka, O. Fouche, E. Freysz and J.-F. Letard, *Chem. Commun.,* 2008, 4327. (b) F. Volatron, L. Catala, E. Riviere, A. Gloter, O. Stephan and T. Mallah, *Inorg. Chem.,* 2008, **47**, 6584. (c) I. Boldog, A. B. Gaspar, V. Martinez, P. Pardo-Ibanez, V. Ksenofontov, A. Bhattacharjee, P. Gütlich and J. A. Real, *Angew. Chem. Int. Ed.,* 2008, **47**, 6433. (d) L. Catala, F. Volatron, D. Brinzei and T. Mallah, *Inorg. Chem.,* 2009, **48**, 3360. (e) M. S. Alam, M. Stocker, K. Gieb, P. Müller, M. Maryono, K. Student and A. Grohmann, *Angew. Chem. Int. Ed.,* 2010, **49**, 1159.

6 (a) O. Roubeau, A. Colin, V. Schmitt and R. Clérac, *Angew. Chem. Int. Ed.,* 2004, **42**, 3399. (b) T. Fujigaya, D.-L. Jiang and T. Aida, *Chem. Asian. J.,* 2007, **2**, 2755. (c) P. Grondin, O. Roubeau, M. Castro, H. Saadaoui, A. Colin and R. Clerac, *Langmuir,* 2010, **26**, 5184. (d) K. Kuroiwa, H. Kikuchi and N. Kimizuka, *Chem. Commun.,* 2010, **46**, 1229.

7 (a) E. Coronado, J.R. Galan-Mascaros, M. Monrabal-Capilla, J. Garcia-Martinez and P. Pardo-Ibanez, *Adv. Mater.,* 2007, **19**, 1359. (b) H. Matsukizono, K. Kuroiwa and N. Kimizuka, *J. Am. Chem. Soc.,* 2008, **130**, 5622. (c) C. Gandolfi, C. Moitzi, P. Schurtenberger, G. G. Morgan and M. Albrecht, *J. Am. Chem. Soc.,* 2008, **130**, 14434.

8 We are not aware of studies on the self-assembly of SCO-active manganese complexes other than Prussian blue analogues (*e.g.* $Rb_xMn[Fe(CN)_6]_y$), in which the spin transition is associated with a metal-to-metal electron transfer, see for examples: (a) S. Cobo, R. Fernandez, L. Salmon, G. Molnar and A. Bousseksou, *Eur. J. Inorg. Chem.,* 2007, 1549; (b) S. Ohkoshi, H. Tokoro and K. Hashimoto, *Coord. Chem. Rev.,* 2005, **249**, 1830. A study on single molecular spin transition, which obviously cannot be cooperative, has appeared recently: (c) E. A. Osorio, K. Moth-Poulsen, H. S. J. van der Zant, J. Paaske, P. Hedegård, K. Flensberg, J. Bendix and T. Bjørnholm, *Nano Lett.,* 2010, **10**, 105.

9 Y. Garcia and P. Gütlich, *Top. Curr. Chem.,* 2004, **234**, 49.

10 (a) A. H. Cooke and H. J. Duffies, *Proc. Phys. Soc. London. Sect. A,* 1955, **A68**, 32. (b) I. D. Charles and M. J. Frank, *J. Inorg. Nucl. Chem.,* 1970, **32**, 555. (c) S. Sen, S. Mitra, D. Luneau, M. S. El Fallah and J. Ribas, *Polyhedron,* 2006, **25**, 2737. (d) F. Hossain, M. A. Rigsby, C. T. Duncan, P. L. Milligan, R. L. Lord, M. Baik and F. A. Schultz, *Inorg. Chem.,* 2007, **46**, 2596.

11 (a) V. V. Zelentsov and I. K. Somova, *Zh. Obshch. Khim.,* 1974, **44**,1309. (b) P. G. Sim and E. Sinn, *J. Am. Chem. Soc.,* 1981, **103**, 241. (c) L. Kaustov M. E. Tal, A. I. Shames and Z. Gross, *Inorg. Chem.,* 1997, **36**, 3503. (d) Y. Garcia, O. Kahn, J.-P. Ader, A. Buzdin, Y. Meurdesoif and M. Guillot, *Phys. Lett. A*, 2000, **271**, 145. (e) M. Nakano, G. Matsubayashi and T. Matsuo, *Phys. Rev. B,* 2002, **66**, 212412. (f) M. Nakano, G. Matsubayashi and T. Matsuo, *Adv. Quantum. Chem.,* 2003, **44**, 617. (g) P. Przychodzen, K. Lewinski, M. Balanda, R. Pelka, M. Rams, T. Wasiutynski, C. Guyard-Duhayon and B. Sieklucka, *Inorg. Chem.,* 2004, **43**, 2967. (h) S. Kimura, Y. Narumi, D. Kindo, M. Nakano and G. Matsubayashi, *Phys. Rev. B,* 2005, **72**, 064448. (i) Y. Garcia, H. Paulsen, V. Schuenemann, A. X. Trautwein and J. A. Wolny, *Phys. Chem. Chem. Phys.,* 2007, **9**, 1194. (j) Z. Liu, S. Liang, X. Di and J. Zhang, *Inorg. Chem. Commun.,* 2008, **11**, 783.

12 G. G. Morgan, K. D. Murnaghan, H. Müller-Bunz, V. McKee and C. J. Harding, *Angew. Chem. Int. Ed.,* 2006, **45**, 7192.

13 C. Gandolfi, N. Miyashita, D. Kurth, P. N. Martinho, G. G. Morgan and M. Albrecht, *Dalton Trans.,* 2010, **39**, 4508.

14 A. Panja, N. Shaikh, S. Gupta, R. J. Butcher and P. Banerjee, *Eur. J. Inorg. Chem.,* 2003, 1540.

15 (a) S. Inoue, T. Yanai, S. Ando, A. Nakazawa, K. Honda, Y. Hoshino and T. Asai, *J. Mater. Chem.,* 2005, **15**, 4746. (b) P. Zell, F. Mögele, U. Ziener and B. Rieger, *Chem. Eur. J.,* 2006, **12**, 3847. (c) I; Aiello, M., Ghedini, M. La Deda, D. Pucci and O. Francescangeli, *Eur. J. Inorg. Chem.,* 1999, 1367.

16 (a) B. D. Sarma, K. R. Ray, R. E. Sievers and J. Bailar, C. *J. Am. Chem. Soc.,* 1964, **86**, 14. (b) A. Panja, N. Shaikh, R. J. Butcher and P. Banerjee, *Inorg. Chim. Acta,* 2003, **351**, 27. (c) M. Bera, K. Biradha and D. Ray, *Inorg. Chim. Acta,* 2004, **357**, 3556.

17 Magnetic measurements on complexes **4** and **5** in solution using Evans' method indicated μ_{eff} values between 4.74 and 4.82 μ_B at RT, thus pointing to the presence of high-spin complexes only. Therefore, spectroscopic properties have been assigned to specific complexes rather than to a spin-equilibrated mixture.

18 Under identical conditions, the unfunctionalized complex [Mn(sal$_2$bapen)]NO_3 displays $E_{1/2}$ = +0.77. This expected slightly higher potential in the absence of alkoxy substituents together with calculations on the unfunctionalized complex, which predict that the HOMO is largely metal-centered,[14] may support the notion that the oxidation observed here is indeed metal-centered.

19 H.-L. Zhu, Y.-X. Tong, X.-L. Yu and X.-M. Chen, *J. Coord. Chem.,* 2002, **55**, 843.

20 M. Hoogenraad, K. Ramkisoensing, S. Gorter, W. L. Driessen, E. Bouwman, J. P. Haasnoot, J. Reedijk, T. Mahabiersing and F. Hartl, *Eur. J. Inorg. Chem.,* 2002, 377.

21 See the electronic supporting information for further details.

22 Further cooling of complex **5c** to 3 K revealed an abrupt drop to 1.54 μ_B, indicating antiferromagnetism below 20 K. Since the inverse susceptibility χ^{-1} is not linear over the measured temperature range, data fitting to the Curie-Weiss law was precluded.

23 The magnetic moment for complex **I** is $\mu_{\text{eff}} = 4.4$ μ_B at 300 K.

24 Y. Bodenthin, G. Schwarz, Z. Tomkowicz, T. Geue, W. Haase, U. Pietsch and D. G. Kurth, *J. Am. Chem. Soc*., 2009, **131**, 2934.

25 Sample annealing may be another process to account for the different magnetic behavior of warmed **5c**. Gradual desolvation in this temperature range has been ruled out by thermogravimetric analyses, which do not show any weight loss up to 80 °C.

26 Similar stabilization of LS states with long alkyl chains has been shown previously with Co(III) and Fe(II) complexes and has been associated with crystal-melt phase transitions, see: (a) S. Hayami, K. Danjobara, K. Inoue, Y. Ogawa, N. Matsumoto and Y. Maeda, *Adv. Mater*., 2004, **16**, 869. (b) M. Seredyuk, A. B. Gaspar, V. Ksenofontov, Y. Galyametdinov, J. Kusz and P. Gütlich, *J. Am. Chem. Soc.,* 2008, **130**, 1431. (c) D. Kiriya, H.-C. Chang and S. Kitagawa, *J. Am. Chem. Soc.,* 2008, **130**, 5515.

27 M. Marchivie, P. Guionneau, J.-F. Letard and D. Chasseau, *Acta Cryst.,* 2005, **B61**, 25.

28 R. Pritchard, S. A. Barrett, C. A. Kilner and M. A. Halcrow, *Dalton Trans.,* 2008, 3159.

29

29 (*a*) R. Rudert, B. Schulz, G. Reck, D. Vollhardt and J. Kriwanek, *Acta Cryst.,* 2000, **B56**, 124. (*b*) S. Abrahamsson, B. Dahlen, H. Löfgren and I. Pascher, *Prog. Chem. Fats Other Lipids,* 1978, **16**, 125.

30 The shortest distance is for **3a** is slightly less than the closest Mn···Mn distance in the spin-stable trien analog of complex **I**, *viz.* [Mn(3-OMe-sal$_2$trien)]NO_3, is 7.814 Å and hence also considerably shorter than in **5a**.

31 A. Ulman, *An Introduction to Ultrathin Organic Films From Langmuir-Blodgett to Self-Assembly*, Academic Press, San Diego, USA, 1991.

32 For examples, see: (a) A. Ruaudel-Teixier, A. Barraud, P. Coronel and O. Kahn, *Thin Solid Films,* 1988, **160**, 107. (b) P. Coronel, A. Barraud, R. Claude, O. Kahn, A. Ruaudel-Teixier and J. Zarembowitch, *J. Chem. Soc., Chem. Commun.,* 1989, 193. (c) O. Kahn, F. Armand, C. Badoux, P. Bonville and A. Ruaudel-Teixier, *Langmuir,* 1995, **11***,* 3467. (d) H. Soyer, C. Mingotaud, M.-L. Boillot and P. Delhaes, *Langmuir,* 1998, **14**, 5890. (e) J. T. Culp, J.-H. Park, D. Stratakis, M. W. Meisel and D. R. Talham, *J. Am. Chem. Soc.,* 2002, **124**, 10083. (f) O. Roubeau, B. Agricole, R. Clerac and S. Ravaine, *J. Phys. Chem. B,* 2004, **108**, 15110. (g) Y. Bodenthin, U. Pietsch, H. Möhwald and D. G. Kurth, *J. Am. Chem. Soc.,* 2005, **127**, 3110. (h) J. A. Kitchen, N. G. White, C. Gandolfi, M. Albrecht, G. N. L. Jameson, J. L. Tallon and S. Brooker, *Chem. Commun.,* 2010, **46**, 6464.

33 (a) D. R. Talham, *Chem. Rev.,* 2004, **104**, 5479. (b) P. M. Mendes, A. H. Flood and J. F. Stoddart, *Appl. Phys. A,* 2005, **80**, 1197. (c) O. Kahn, *Molecular Magnetism*, VCH, New York, USA, 1993. (d) C. Mingotaud, P. Delhaes, M. W. Meisel and D. R. Talham, in *Magnetism: Molecules to Materials II,* J. S. Miller and M. Drillon (eds.), Wiley-VCH, Weinheim, Germany, 2002, p 457. (e) P. Gütlich, Y. Garcia and H. Spiering, in *Magnetism: Molecules to Materials IV*, J. S. Miller and M. Drillon (eds.), Wiley-VCH, Weinheim, Germany, 2002, p 271. (f) I. Prieto, M. T. Martin and L. Camacho, in *Nanoscale Materials*, L. M. Liz-Marzan and P. V. Karmat (eds.), Springer, USA, 2003, p 303.

34 A possible rationale for this behavior may rely on the severe distortion of the octahedral coordination geometry around the manganese center, which imposes a certain coordinative flexibility. Upon compression, the transoid arrangement may be less rigid and may allow for interdigitation of alkyl chains of neighboring complexes. Such interdigitation may build up considerable tension, which is in agreement with the low stability of the formed films.

35 E. R. T. Tiekink and J. J. Vittal (eds.), *Frontiers in Crystal Engineering*, John Wiley & Sons, Chichester, UK, 2006.

36 (a) Z. Guo, T. Jiao and M. Liu, *Langmuir,* 2007, **23***,* 1824. (b) R. Aveyard, B. P. Binks, N. Carr, A. W. Cross, G. W. Gray, P. W. A; Kilvert and D. Lacey, *Colloids Surf.,* 1992, **65**, 29.

37 (a) P. U. Muller, E. Weber, G. Rheinwald and W. Seichter, *Org. Biomol. Chem.,* 2005, **3**, 3757. (b) P. Muller, C. C. Akpo, K. W. Stockelhuber and E. Weber, *Adv. Colloid Interface Sci.,* 2005, **114**, 291. (c) N. Reitzel, D. R. Greve, K. Kjaer, P. B. Howes, M. Jayaraman, S. Savoy, R. D. McCullough, J. T. McDevitt and T. Bjørnholm, *J. Am. Chem. Soc.,* 2000**, 122***,* 5788.

38 N. G. Connelly and W. E. Geiger, *Chem. Rev.,* 1996, **96**, 877.

39 Determined using the ferrocenium/ferrocene (Fc+/Fc) couple.

40 Identical plots were obtained for **5c** irrespective of whether the measurement was performed under an applied field of 0.1 T or 1 T.

41 G. M. Sheldrick, *Acta Cryst.,* 2008*,* **A64**,112.

42 A. L. Spek, *J. Appl. Crystallogr.,* 2003, **36**, 7.

43 H. D. Flack, *Acta Cryst.,* 1983*,* **A39**, 876.

for Table of Contents use only

Synthesis and Self-Assembly of Spin-Labile and Redox-Active Manganese(III) Complexes

C. Gandolfi, T. Cotting, P. N. Martinho, O. Sereda, A. Neels, G. G. Morgan, M. Albrecht*

Amphiphilic functionalization of manganese(III) complexes induces spin crossover and promotes self-assembly in the solid state and at the air-water interface.